

MODEL CALCULATIONS OF THE MULTIPLE SCATTERING FOR THE DEPOLARIZATION RATIOS BY POLARIZATION LIDAR MEASUREMENTS

Hiroshi Ishimoto*, Kazuhiko Masuda, and Takahisa Kobayashi
 Meteorological Research Institute, Nagamine 1-1, Tsukuba 305-0052, Japan

1. Introduction

Depolarization measurements by polarization lidar are useful to know the existence of crystal particles in the clouds. For the scattering of single particle, the depolarization for spherical particles is zero in all scattering angles while non-spherical particles have some positive values. Furthermore, the values depend on the particles' sizes and shapes. Therefore, the measurements have a potential possibility to obtain the information about the averaged sizes and shapes for the observed crystal particles. Lidar observations can identify the location of the particles which cause the single scattering. Thus, the analyses of the observed depolarization at the specific location in the cloud will be important for the further studies of the ice clouds as well as their microphysics (e.g. Sassen 1991, Sassen 1994).

However, the observed signals of the lidar measurements are not only from those of the single scattering, but a contribution of the multiple scattering may change the values of the observed intensity and depolarization significantly (e.g. Sun et al. 1989, Sassen et al. 1992, Gobbi 1998, Roy et al. 1999). Some factors will make increase the contamination of the multiple-scattered light, such as observed field of view (FOV), optical thickness, and vertical structure in the clouds (e.g. Bissonnette et al. 1995, Kobayashi 1998). In this work, the effects of multiple scattering on the observed depolarization by the ground-based lidar are examined for some simplified cloud models.

2. Numerical methods and modeled environment

For the model calculations, we have developed a numerical code for the calculations of the Stokes parameters based on the Backward Monte Carlo approaches. The basic concept and the performance of the Backward Monte Carlo method for the scalar intensities are described by O'Brien 1992. In addition, a treatment of Forward Monte Carlo method is applied in the terms of the second scattering for the applications to the incident narrow beam (Detailed explanations will be published elsewhere). Up to 20 orders of multiple scattering are taken into

account for the calculations.

Modeled environment and the assumed particles are illustrated in Figs.1-2 and explanations for the cloud particles are denoted in the caption of Fig.2. From the observed scattered light $(I, Q, U, V)^T$ for the normalized linear polarized incident beam $(I_i, Q_i, U_i, V_i)^T = (1, 1, 0, 0)^T$, the depolarization ratio δ is derived by $\delta = (I - Q)/(I + Q)$. The resultant depolarization ratios are plotted as a function of the half of the optical path length of the returned signal, which is named "penetration depth" from the assumption of single scattering for lidar observations.

Since the results of our Monte Carlo calculations derive the discrete values of the penetration depth for each photon and the number of the photons tends to decrease as increase the penetration depth, a numerical averaging is adopted for the raw data of the Monte Carlo calculations. The observed light $g(r)$ with penetration depth r has been attenuated during its optical path length $2r$, therefore, $g(r)$ will be in the form as,

$$g(r) = p(r)e^{-2C_{ext}r}, \quad (1)$$

where $p(r)$ is an unknown function and C_{ext} is the extinction coefficient in the cloud. Applying $x = 2C_{ext}r$, a cumulative function $f(r)$ becomes,

$$f(r) = \frac{1}{2C_{ext}} \int_0^x p(t)e^{-t} dt. \quad (2)$$

If we assume that the function $p(t)$ can be written as $p(t) \sim t^{a-1}$ ($a > 0$),

$$f(r) \propto \int_0^x t^{a-1} e^{-t} dt. \quad (3)$$

After the normalization by the value at the maximum penetration depth r_m ,

$$\begin{aligned} f(r) &\sim f(r_m) \left(\int_0^x t^{a-1} e^{-t} dt \right) / \left(\int_0^{x_m} t^{a-1} e^{-t} dt \right) \\ &= f(r_m) \frac{P(a, x)}{P(a, x_m)}, \end{aligned} \quad (4)$$

where $P(a, x)$ is an *incomplete gamma function*. From the raw dataset $f_r(r)$ of the Monte Carlo results, the parameter a is obtained by using the least squares fitting. The fitting function for $g(r)$ is derived by differentiating the function $f(r)$. Using a *gamma function* $\Gamma(a)$,

$$g(r) \sim \frac{f(r_m)2C_{ext}}{\Gamma(a)P(a, r_m)} (2C_{ext}r)^{a-1} e^{-2C_{ext}r}. \quad (5)$$

Note that such numerical averaging is applicable because we know the value C_{ext} in the modeled clouds. Since we took into account a known dependence of C_{ext} for the raw data of the Monte Carlo results, numerical errors of the resultant depolarization plots are relatively small comparing with the direct plots of the raw data. A sample results for the multiple-to-single scattering intensities in the case of homogeneous C1 cloud is represented in Fig.3 for a comparison with the results by Bissonnette et al. 1995 (fig.2).

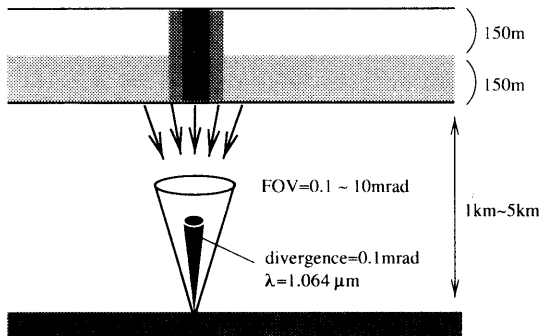


Fig. 1.— Modeled environment for the numerical simulations.

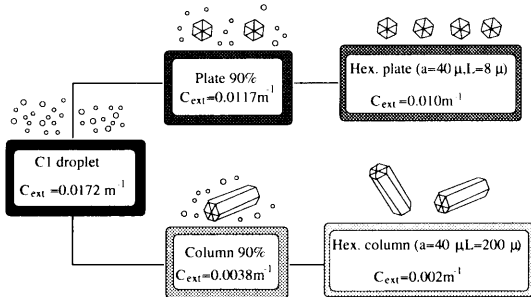


Fig. 2.— Cloud particles applied to the model calculations. For cloud droplets, C1 model (e.g. Deirmendjian 1975) is used for their size distribution and concentration. For the crystal particles, a uniform size is considered for the hexagonal plate (radius $40\mu\text{m}$, width $8\mu\text{m}$) and hexagonal column (radius $40\mu\text{m}$, length $200\mu\text{m}$), respectively. Mie theory and a lay tracing method are used for the volume averaged scattering properties of the droplets and crystals (within 10° of randomized surface distortion and 3-D random orientation are applied for crystal particles). The resultant depolarization ratios at the scattering angle 180° are 0.21 for the hexagonal plates and 0.25 for the hexagonal columns. The averaged extinction coefficients C_{ext} (m^{-1}) are derived assuming a mass conservation for each set of particles in simplicity.

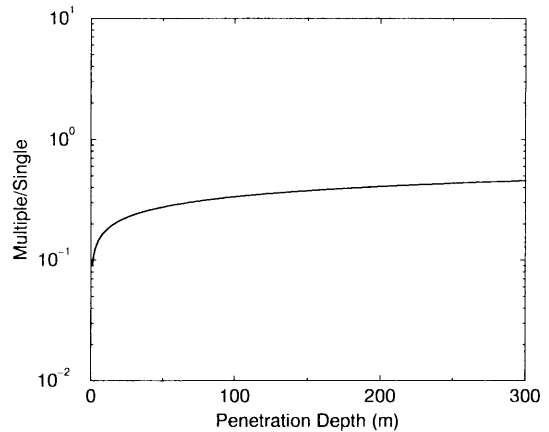


Fig. 3.— Sample results of the multiple-to-single scattering ratios in the case of uniform C1 cloud with $\text{FOV}=1\text{mrad}$. Unpolarized incident beam is adopted for the comparison with Bissonnette et al. 1995.

3. Results of the depolarization ratios

Numerical results of the depolarization ratios δ in different FOV's for the modeled clouds are plotted in Figs.4-6. It should be noted that the difference of the values near the lower boundary (penetration depth ~ 0) for the same cloud between Figs.4-6 is due to the numerical averaging denoted above.

In the case of $\text{FOV}=0.1\text{mrad}$ (Fig.4), the values δ for each cloud don't change significantly as increase the penetration depths. It indicates that the contribution of the multiple scattering is small and the absolute values of the resultant depolarization are almost the same as those of their single scattering. If we assume the mixing between droplets and crystals, the averaged depolarization ratios for the single scattering will be the values in between the pure crystal case and the pure droplets case. Under the assumption of the mass conservation for each particles set, the number of the hexagonal columns in the unit volume is smaller than that of the hexagonal plates due to the considered crystal sizes. Comparing with the case of plate 90% (in mass), therefore, the averaged value of the depolarization for the case of column 90% becomes closer to that of pure C1 droplets.

Since the scattering probability for an incident photon increases as increases the optical thickness in the unit volume of the cloud and the absorption efficiencies of the assumed particles are small, the influence of the multiple scattering is larger for the clouds with higher extinction coefficients. Moreover, the probability to observe the multiple-scattered lights increases as increase the observing FOV. Therefore, the enhancement

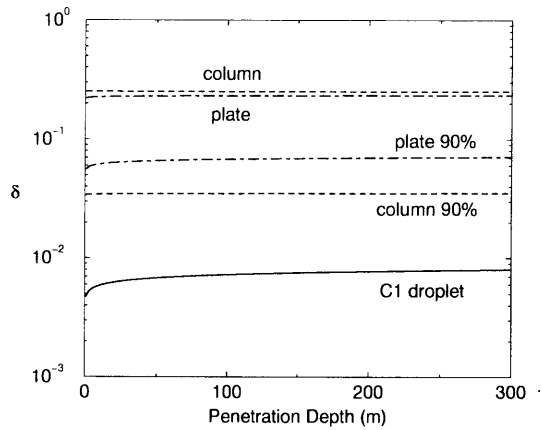


Fig. 4.— Depolarization of the homogeneous clouds as a function of the penetration depth in the case of $\text{FOV}=0.1\text{mrad}$. The cloud base height is settled 1km above the ground base

of the depolarization due to the multiple scattering depends on the clouds' C_{ext} and FOV. As the results, the depolarization owing to the multiple scattering for the droplet layer possibly exceeds the values of the crystal layer. In the case of $\text{FOV}=10\text{mrad}$ (Fig.6), δ for the C1 cloud becomes larger than that in the case of column 90% with the penetration depth longer than 40m, and almost the same order of magnitude as those of the pure crystal clouds around the upper end of the penetration depth. These results indicate a fundamental difficulty to estimate the particles' physical parameters, i.e. shapes and sizes, only from the depolarization measurements with relatively wide FOV.

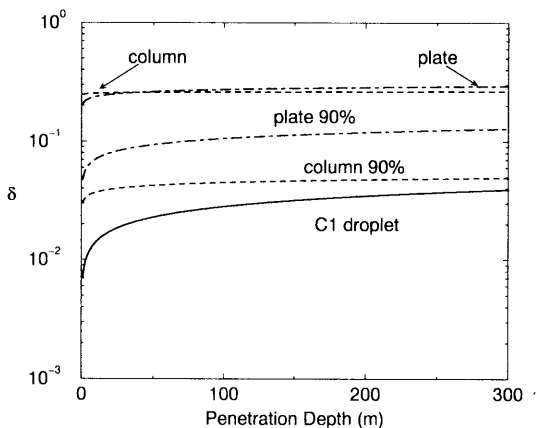


Fig. 5.— Same as Fig.4, but in the case of $\text{FOV}=1\text{mrad}$.

For the next step, the effect of the vertical structure in the cloud is examined. Fig.7 shows the results of the case where we assumed the C1 droplets for the lower half and the hexagonal plates for the upper half in the cloud. As already depicted in Figs.4-6, the values δ become

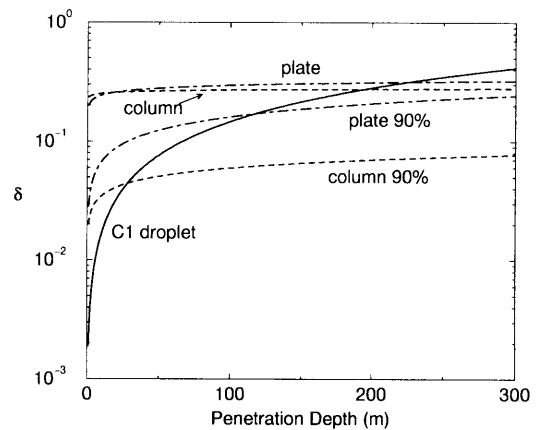


Fig. 6.— Same as Fig.4, but in the case of $\text{FOV}=10\text{mrad}$.

greater as wider the observed FOV in Fig.7. Furthermore, a vertical inhomogeneity in the cloud cause a kind of adjacency effect for the measured depolarization. Since the multiple scattering occurs at the lower part in the cloud than the assumed penetration depth, the signals due to the multiple scattering in the droplets part overlap the scattered light from the crystal part with the same penetration depth. Then, an additional increases for the observed depolarization occurs. In Fig.7, this effect is prominent in the case of $\text{FOV}=10\text{mrad}$ with the penetration depth between 150m and 200m. As longer the penetration depth in the crystal part, the effect of this overlapping decreases because of the attenuation of the multiple-scattered lights in the droplet part. If the multiple scattering in the crystal part is less effective than that in the droplet part, the values δ will decrease as increase the penetration depth and converge to the same values as in the case of homogeneous crystal clouds (see, Fig.6).

The results of our numerical calculations indicate that the values of the depolarization cannot be estimated only from the extinction coefficient of the crystal layer, and the adjacent cloud layer should be taken into account if it exists. Moreover, it indicates that the observed depolarization for the vertically separated cloud will be different from that of the mixing phase even if the bulk crystal ratio in the observed cloud was the same.

In the previous figures, the contributions of the multiple scattering in the case of $\text{FOV}=0.1\text{mrad}$ were almost negligible. However, it is because we have assumed the cloud base height as 1km. Fig.8 is the plots of the depolarization ratio for $\text{FOV}=0.1\text{mrad}$ with the same cloud structure as Fig.7 but in the cases of the different cloud base heights. The increase of the cloud base height

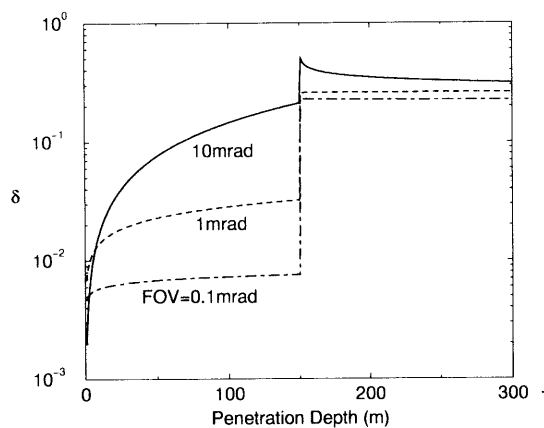


Fig. 7.— Same as Fig.4 but a vertical inhomogeneity (droplets for lower half and hexagonal plate for upper half) is taken into account. The lines denote the cases of the different FOV's.

causes the similar effects as those by the increase of the FOV. Although the assumed cloud situations in Fig.8 may be uncommon, it can be said that the influence of the multiple scattering for the depolarization ratios will be significant in some cases even for the observations with relatively narrow FOV. In particular, observed depolarization for relatively dense clouds with high altitude will be an overestimation for the value of the single scattering of the crystal particles in the clouds.

To estimate the particles sizes or shapes from the observed depolarization ratios, therefore, an analysis to remove the multiple scattering component from the observed data will be important.

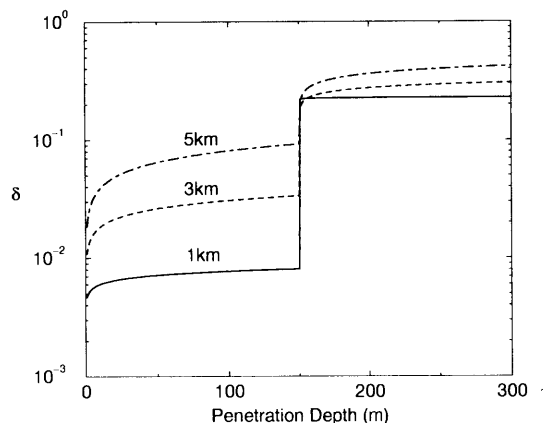


Fig. 8.— Dependence on the cloud base height. FOV is 0.1mrad and the other conditions are the same as Fig.7.

One possibility to estimate the depolarization ratio of the single scattering is to extrapolate the values by multi-FOV observations. Fig.9 is the results of the averaged depolarization with pen-

etration depth from 200m to 250m in the same cloud situation as Fig.8 for different FOV's. As represented in the previous figures, the influence of the multiple scattering for the observed depolarization ratios depends on several factors, such as optical thickness, vertical structure in the cloud, and cloud base height. Therefore, the dependence of the FOV for the observed depolarization will not be described in a simple relationship. However, the values should be converged to those of the single scattering as decrease the FOV, even in some complex cloud situations. Thus, the extrapolated values from the observed trend of the depolarization ratios will be closer to those of the single scattering. Plural observations within relatively narrow FOV's will be important for such extrapolations in the practical analyses.

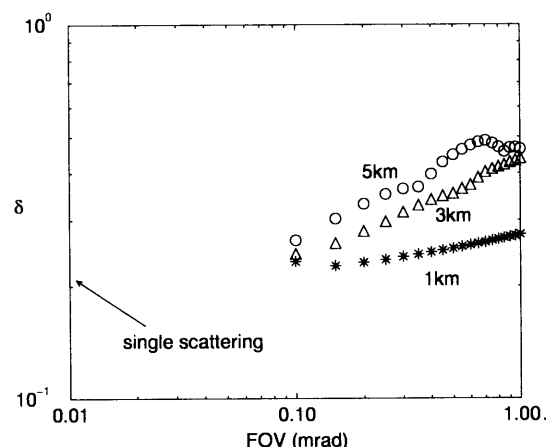


Fig. 9.— Dependence on the FOV for the averaged depolarization ratio with penetration depths from 200m to 250m for the same cloud conditions as Fig.8.

4. Summary

On the basis of the Monte Carlo calculations, the effects of multiple scattering for the polarization lidar measurements are discussed in some simplified cloud models. The mixing of the multiple-scattered light in the returned signals enhance their depolarization ratios from those of the single scattering. The contributions of the multiple-scattered light depend strongly on the observed FOV's and the extinction coefficients in the clouds. Furthermore, vertical inhomogeneities in the clouds, such as the existence of an adjacent dense droplets layer, raise the values of the depolarization ratio at the the crystal layer of the penetration depth. If we observe a cloud with narrow FOV, the influence of the multiple scattering is relatively small. However, the measured depolarization ratios may change in differ-

ent cloud base height even if the cloud itself was the same. Considering the complex structures and dynamics of the clouds, direct interpretation from the single FOV observations may cause a overestimation for the particles' sizes or shapes in some cases of the clouds. Moreover, the model calculations of the multiple scattering for the observed depolarization ratios may be ineffective to retrieve the particles' detailed information, because of the various parameters denoted above. On the contrary, the depolarization ratios which estimated indirectly by the multi-FOV observations will be reliable for the values of the single scattering, though it may difficult to confirm the mixing phases between droplets and crystals because of the small values of their depolarization ratios (see, Fig.4). From the extrapolated values of the depolarization ratios for single scattering, it is expected to know the detailed information about the nature and the microphysics of the ice clouds.

REFERENCES

- Bissonnette, L. R., et al. 1995. LIDAR multiple scattering from clouds. *Appl. Phys. B*, **60**, 355-362.
- Deirmendjian, D. 1975. Far-infrared and sub-millimeter wave attenuation by clouds and rain. *J. Appl. Meteorol.*, **14**, 1584-1593.
- Gobbi, G. P. 1998. Polarization lidar returns from aerosols and thin clouds: a framework for the analysis. *Applied Optics*, **37**, 5505-5508.
- Kobayashi, T. 1998. Multiple scattering effects on the space-borne lidar signals. *J. of Remote Sensing Society of Japan*, **18**, 2-11.
- O'Brien, D. M. 1992. Accelerated quasi Monte Carlo integration of the radiative transfer equation. *J. Quant. Spectrosc. Radiat. Transfer*, **48**, 41-59.
- Roy, G., L. Bissonnette, C. Bastille, and G. Vallée 1999. Retrieval of droplet-size density distribution from multiple-field-of-view cross-polarized lidar signals: theory and experimental validation. *Applied Optics*, **38**, 5202-5211.
- Sassen, K. 1991. The polarized lidar technique for cloud research: A review and current assessment. *Bull. Amer. Meteor. Soc.*, **72**, 1848-1866.
- Sassen, K., H. Zhao, and G. C. Dodd 1992. Simulated polarization diversity lidar returns from water and precipitating mixed phase clouds. *Applied Optics*, **31**, 2914-2923.
- Sassen, K. 1994. Advances in polarization diversity lidar for cloud remote sensing. *Proc. IEEE*, **82**, 1907-1914.
- Sun, Y.-Y., Z.-P. Li, and J. Bösenberg 1989. Depolarization of polarized light caused by high altitude clouds. 1: Depolarization of lidar induced by cirrus. *Applied Optics*, **28**, 3625-3632.

Corresponding author address: Hiroshi Ishimoto, Meteorological Research Institute, Japan Meteorological Agency, Nagamine 1-1, Tsukuba 305-0052, Japan
e-mail: hishimot@mri-jma.go.jp